Neuroscience Vol. 15, No. 1, pp. 1–12, 1985
Printed in Great Britain

0306-4522/85 $3.00 + 0.00
Pergamon Press Ltd
© 1985 IBRO

DEPOLARIZING AFTERPOTENTIALS IN MYELINATED AXONS OF MAMMALIAN SPINAL CORD

A. R. BLIGHT and S. SOMEYA
Departments of Neurosurgery and Physiology and Biophysics, New York University Medical Center, 550 First Avenue, New York, NY 10016, U.S.A.

Abstract—Microelectrode recordings were made from 5–10 μm dia axons of adult rat spinal cord *in vitro*. Action potentials in response to electrical stimulation were recorded intracellularly and electrical characteristics of the axons were examined by injecting current pulses through a bridge circuit. All action potentials larger in amplitude than 80 mV were followed by depolarizing afterpotentials, similar to those recorded in peripheral axons [Barrett and Barrett (1982) *J. Physiol., Lond.* **323**, 117–144].

The afterpotential could be described as the sum of three exponential components, the time constants of which (τ_1, τ_2 and τ_3) were 25.2 ± 5.6, 3.1 ± 0.8 and 0.8 ± 0.3 ms, respectively, at 25°C and a membrane potential of -80 mV. The maximal amplitudes of the afterpotential components, obtained by extrapolating to the peak of the action potential, were 3.8 ± 1.0, 6.4 ± 5.2 and 21.7 ± 9.8 mV, for action potential amplitudes of 102 ± 11 mV. The amplitude of the longest component of the afterpotential decreased with depolarization and increased with hyperpolarization at the recording site. The amplitude decreased markedly with increase of temperature to physiological levels, in conjunction with the expected decrease in action potential duration. Similar afterpotential components were present in the response of the axon to injected hyperpolarizing current pulses.

The observations are consistent with the suggestion [Barrett and Barrett (1982) *J. Physiol., Lond.* **323**, 117–144] that the afterpotential results from charging of the axolemmal capacitance by current passing through the myelin sheath during the action potential. They are inconsistent with a number of calculations of electrical characteristics of peripheral axons derived from voltage clamp experiments in isolated fibers. It is argued that the electrical resistance of the myelin lamellae is relatively low, though within the range calculated for other glial membranes. This suggestion is found more compatible with the available morphological data than the alternative proposal that a leakage pathway under the myelin sheath might be responsible for the afterpotential [Barrett and Barrett (1982) *J. Physiol., Lond.* **323**, 117–144]. The significance of this organization for the function of myelinated axons and the electrical basis of the afterpotential are examined further in the accompanying paper [Blight (1985) *Neuroscience* **15**, 13–31].

Physiological studies of saltatory conduction in myelinated axons have concentrated on the function of the nodal membrane (reviewed in Refs 18, 20, 49 and 51). Relatively little is known about the biophysical characteristics of the internode.[1,13,39,50] There is no detailed understanding of the effect of myelin sheath properties on saltatory conduction. Most speculation in this area has relied on computer simulations[9,15,17,27,29,43,45,53] that are limited by the paucity of quantitative data.

The general assumption, since the original "submarine cable" analogy of Ranvier,[36] has been that the myelin sheath represents a high-impedance shield around the internode that reduces the radial leakage of current. Its role in minimizing the capacitative current and reducing the time constant of the axon was emphasized later,[41] but remains less intuitively obvious. Barrett and Barrett,[1] in a study of intracellular recording from vertebrate (mostly poikilothermic) peripheral axons, reached the revolutionary conclusion that there is a low-resistance pathway through the myelin sheath. The proposition of such a pathway was necessary to account for the presence of large, prolonged depolarizing afterpotentials. It was suggested that these potentials were due to partial charging of the internodal axonal membrane capacitance during the action potential, followed by passive discharge with a time constant of the order of 100 ms. This interpretation calls into question the concept of the myelin sheath as an insulator, and even as a modulator of capacitance.

The present work describes intracellular recordings from myelinated axons of the mammalian spinal cord, using an isolated spinal tract preparation previously developed for the cat.[5] Most of the data reported here were obtained from rats, though qualitatively similar observations were also made in the cat spinal cord. Some quantitative differences were found between these species. The interpretation of the origin and significance of afterpotentials in myelinated axons, begun here, is dealt with more fully in the succeeding paper,[7] with the aid of computer modelling. A preliminary report of these findings was published in abstract form.[6]

EXPERIMENTAL PROCEDURES

The in vitro *spinal cord*

All recordings were made from spinal cord tracts *in vitro* largely using Sprague–Dawley rats, but some observations

Please address all correspondence to: A. R. Blight.

were confirmed in the cat. Procedures for the cat are described elsewhere.[5]

Adult rats of 200–300 g body weight were anaesthetized with sodium pentobarbital (40 mg/kg). The vertebral column was exposed from the dorsal side and excised rapidly, cutting through the upper cervical and lower lumbar level with scissors. It was then immersed for several seconds in cold (5–10°C) Krebs solution and the cord exposed by laminectomy, cutting through the lateral walls of the vertebrae with scissors. The cord was removed from the vertebral column and placed in flowing, oxygenated Krebs solution. The dura was removed and an incision of the pia was made along the length of the ventral spinal artery. The cord was hemisected by cutting vertically through the incision with a scalpel blade. The sagittal halves of the cord were then similarly bisected horizontally to give two ventrolateral and two dorsolateral strips of cord from midcervical to midlumbar levels (Fig. 1).

The isolated tracts were transferred to 20 ml vials of Krebs solution, bubbled continuously with 95% O_2, 5% CO_2 at room temperature. They were left for at least 2 h before recording. Most recordings were obtained between 2 and 14 h after removal, though similar results were obtained after more than 24 h *in vitro*. The tract selected for recording was transferred to the recording chamber, consisting of a channel cut in a plexiglass block, along which solutions were perfused (Fig. 1).

The composition of the Krebs solution was the following:[28,56] NaCl 124 mM; KCl 5 mM; K_2HPO_4 1.2 mM; $MgSO_4$ 1.3 mM; $NaHCO_3$ 26 mM; $CaCl_2$ 2.4 mM; Dextrose 20 mM. This solution was equilibrated with 95% O_2, 5% CO_2 at pH 7.2–7.4. A small amount of the indicator Phenol Red was used to monitor the pH during superfusion.

Intracellular recording

Microelectrode recordings were made using glass capillaries filled with 2–3 M KCl, having resistances in the range of 20–30 MΩ. A bridge amplifier (Neurodata Instruments, New York) was used to record and inject current. The capacity neutralization was adjusted to the optimum for maintenance of the square calibration pulse, without oscillation. Data were monitored with a digital oscilloscope and stored and plotted with a digital data acquisition and storage device (Bascom-Turner Instruments 8120 recorder), which was also used to derive the semilogarithmic plots. The digitized plots were analysed by computer, using least squares analysis for determination of log slopes.

Axons were stimulated at a distance from the recording site by means of bipolar wire electrodes (Fig. 1) connected to a pulse-generator through conventional isolation units (WP Instruments). Stimulation was normally by 0.1 ms monophasic pulses of constant current, the cathode nearer to the recording site. The temperature of the recording bath was controlled by a thermoelectric (Peltier) unit, with feedback control from a thermistor located near the middle of the tract.

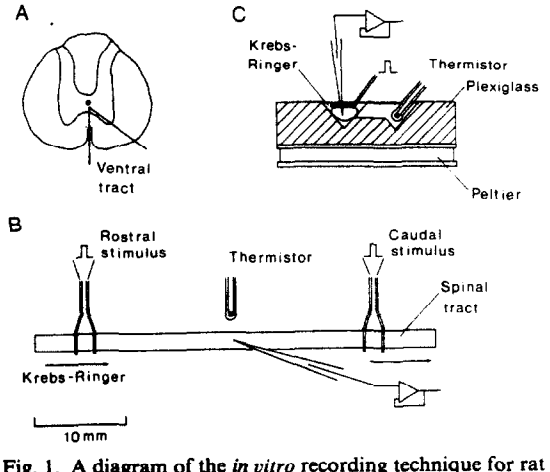

Fig. 1. A diagram of the *in vitro* recording technique for rat spinal cord. All recordings reported here were made from the ventral tracts, cut at an angle (A) to minimize the inclusion of gray matter. The ventral tract was placed in a groove in the recording chamber and held lightly with two bipolar stimulating electrodes near the ends (B, C). Recordings were made near the middle of the tract (thoracic region). The tissue was superfused with Krebs solution and its temperature monitored and controlled with a thermistor and Peltier unit.

RESULTS

Criteria for selection of recordings

Recordings were made from many hundreds of axons in 78 rats during the course of this study and the limited data presented here were selected on strict criteria for intra-axonal recording. The great majority of axons in the spinal cord are too small to be penetrated successfully by the microelectrode. Successful intracellular recordings from larger fibers were indicated by initial sudden baseline shifts of more than 50 mV, accompanied by action potentials from 40–70 mV which clearly increased in amplitude with small hyperpolarizing currents (<4 nA) to values between 70 and 120 mV. Less frequently, recordings of large amplitude action potentials were made without a baseline shift. These were interpreted as recordings from within the myelin sheath, following the conclusions of previous reports.[1,55] In these cases it was often possible to push further into the fiber and obtain a clear baseline shift and intra-axonal recording.

These data indicated that even in the best of recordings there was considerable current leak around the electrode impalement, as is usually the case with intra-axonal recording in mammals.[26,55] This meant that afterpotentials, which are quite dependent on membrane polarization, could only be studied when the resting potential of the axon was supported by hyperpolarizing current. The recordings selected for presentation and analysis here were from those selected axons which showed clear resting potentials, which could be held at a stable membrane potential of −80 mV by hyperpolarizing current (a potential which was always confirmed by a sharp baseline shift on withdrawing the electrode at the end of the recording) and which conducted action potentials from the stimulating electrodes. The recorded amplitude of these action potentials was larger than 80 mV, with a level of amplifier capacity neutralization that was insufficient to restore the full amplitude of the rising phase of the spike.

The propagated action potential

The form of the recorded action potential, generated by distant electrical stimulation, is illustrated in Fig. 2. For all action potentials larger than 80 mV in

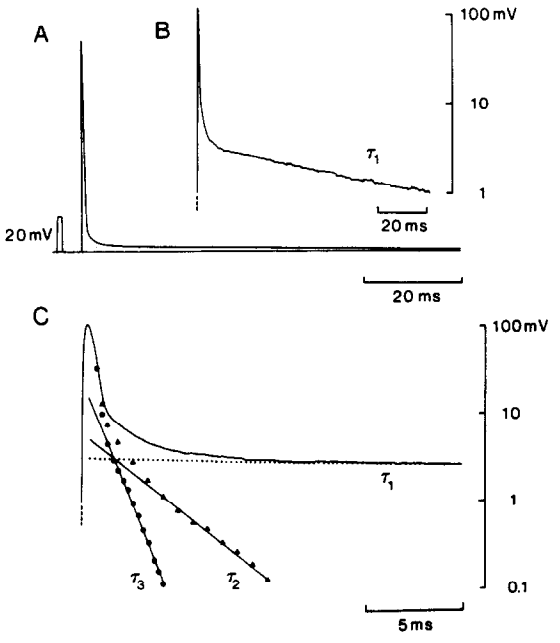

Fig. 2. The form of the action potential recorded in spinal axons, showing an example with a particularly long time constant. (A) An averaged record of 10 spikes, showing the prolonged after-depolarization compared with the baseline. The same record is plotted on a semilog scale in (B), to show the exponential nature of the later part of the relaxation. (C) The earlier part of the afterpotential is divisible into a least three exponential components ($\tau_{1\text{-}3}$) by "peeling" from the semilog plot. The dotted line (τ_1) represents the extension of the log slope seen in (B). The triangles show the result of subtracting the τ_1 component from the original record, and the line (τ_2) indicates the second exponential component. The filled circles represent the result of subtracting τ_1 and τ_2 from the original record. The third exponential component (τ_3) merges into the falling phase of the action potential itself.

amplitude, a depolarizing afterpotential of long duration was found to follow the spike. It could be separated into a series of exponential components by "peeling" from the semilog plots (e.g. Ref. 35). The time constants of these components can be obtained by dividing $\log_{10} e$ by the semilog slopes. Three of these components could be measured accurately. The possibility of longer components of small amplitude could not be addressed because of the limited voltage resolution, and shorter time constants could not be measured accurately because of the limited frequency response of the microelectrode recordings. The maximal amplitude of the different components was estimated by extrapolating the semilog slopes of the afterpotential to the time of the peak of the action potential (Fig. 2 and Tables 1 and 2).

Effect of polarization

The form of the afterpotential was found to be dependent on the local membrane polarization and the temperature. The effect of raising and lowering the membrane resting potential by injection of current through the electrode is shown in Fig. 3. At more depolarized levels the longest component of the afterpotential is small in amplitude and difficult to resolve. With hyperpolarization the afterpotential is increased in amplitude, as is the action potential itself. Some of these data are shown numerically in Table 2. The time constant (τ_1) of the afterpotential was changed only slightly by the same shifts of polarization. Both the amplitude and the time constant of the τ_2 component were less affected. The shortest component decreased in time constant (τ_3) and increased in amplitude with hyperpolarization.

As the characteristics of the afterpotential depend on polarization, it was important to control this parameter. Recordings at a resting membrane potential of −80 mV are given in Table 1. This potential was set by current injection through the electrode and was selected on the basis of interpretations of the normal nodal resting potential from voltage clamp studies of the peripheral axon.[10,14,31]

Amplifier bridge balance

Accurate measurement of resting potential with injected current depended on the ability to balance the bridge of the amplifier. This can be made difficult by pulse artefacts, given the short time constants of the membrane response in the axon. A check on the bridge balance was provided in these cases by reference to the peak of the action potential during injection of a depolarizing current pulse. The spikes generated by distant stimulation and by current

Table 1. Parameters of the recorded action potential in rat spinal (ventral tract) axons at 25°C and −80 mV resting membrane potential ($n = 22$)

	Mean	SD	Units
Spike amplitude	102	11	mV
Component 1			
Time constant (τ_1)	25.2	5.6	ms
Peak amplitude	3.8	1.0	mV
Component 2			
Time constant (τ_2)	3.1	0.8	ms
Peak amplitude	6.4	5.2	mV
Component 3			
Time constant (τ_3)	0.8	0.3	ms
Peak amplitude	21.7	9.8	mV

Table 2. Time constant and amplitude of afterpotential components at different resting membrane polarizations (see Fig. 3)

Afterpotential component	Resting membrane polarization (mV) −67	−77	−87	
τ_1	19.6	21.2	21.6	ms
τ_1 amplitude	2.1	3.6	4.5	mV
τ_2	3.7	3.6	3.5	ms
τ_2 amplitude	4.6	5.1	5.4	mV
τ_3	1.6	1.4	1.1	ms
τ_3 amplitude	4.6	9.5	16.8	mV

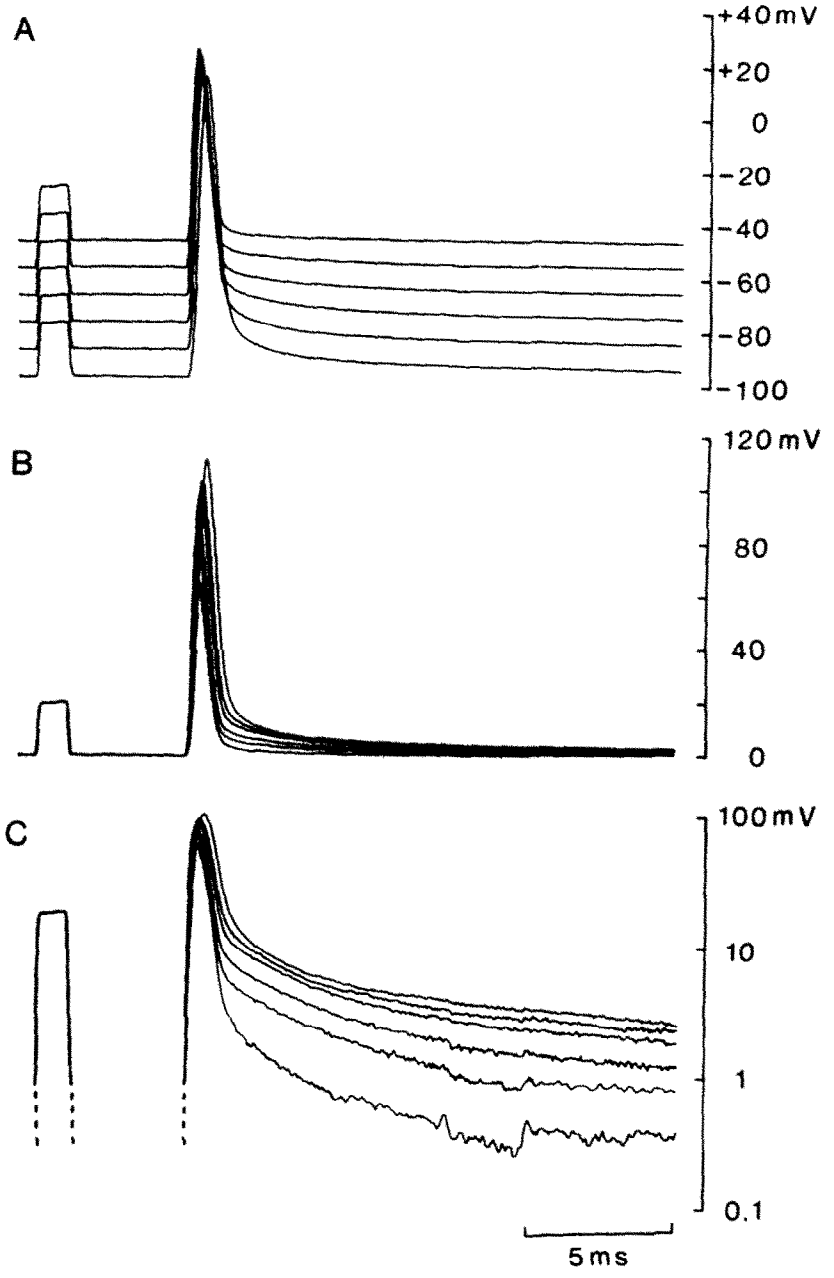

Fig. 3. The amplitude of the afterpotential is dependent on the resting membrane potential at the recording site. This figure shows three different superimpositions of the same sequence of action potentials recorded at different membrane potentials. The records are superimposed relative to the actual resting potentials (A), and with respect to their baselines (B). Semilogarithmic plots are given in (C), to show that the longest time constant is little affected, whilst the amplitude changes by almost an order of magnitude. Note that the peak of the spike is delayed by hyperpolarizing below 90 mV. (See also Table 2.)

injected through the electrode are shown in Fig. 4(A) to reach comparable peaks when the bridge is balanced. This technique is not reliable where there is a small action potential due to inadequate transmission at nearby nodes. Under these conditions, the amplitude of the action potential may vary considerably with the input resistance seen by the node. The match was found to be consistent in this study for units with large amplitude action potentials, inasmuch as the peak of the spike remained at a similar level as the amplitude of the current pulse was raised, or when the current pulse was shortened such that the spike peak occurred after the termination of the current injection (Fig. 4B).

Effect of temperature

With increase of temperature towards physiological levels, the amplitude of the afterpotential

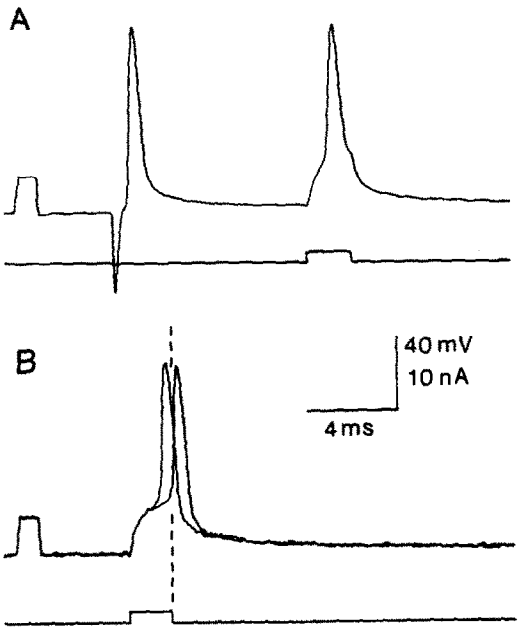

Fig. 4. Illustrations of amplifier bridge-balancing, to show that the peak of the action potential remains close to the same level during a depolarizing current pulse. In (A) the first spike was elicited by distant electrical stimulation and the second by injection of a short current pulse through the recording electrode (bottom trace). The amplifier bridge was adjusted and the peaks of the two spikes were close to the same level. Balancing on the shape of the pulse is sometimes difficult because of the short time constants of the axon, and the spike peak can be used to check the accuracy of the balance. In (B) a threshold current pulse was injected through the electrode and on two separate sweeps the action potentials occurred just before or just after the pulse termination. The later spike is a little depressed in this case, probably because of the slower rate of rise of potential at the node.

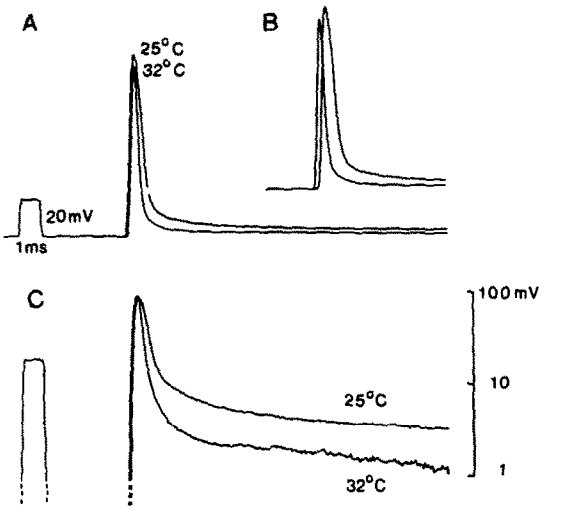

Fig. 5. The effect of temperature on the afterpotential. In another axon, the effect of raising the temperature of the bath is illustrated, again with three representations of the same data. In (A) the spikes are shown superimposed relative to their rising phases, to show the decrease in action potential duration and afterpotential amplitude. In (B) the spikes are superimposed relative to the stimulus pulse (not visible in the record) showing that both latency and duration decrease. The semilog plots in (C) indicate the reduction in amplitude rather than time constant of the after potential with increase in temperature.

decreased, in parallel with reductions in the duration of the action potential (Fig. 5). For the data recorded in Table 1, the temperature was held at 25°C to allow comparison with data from other studies, most of which have used similar temperatures (e.g. Refs 1, 5, 10 and 31) or even lower.[14] It should therefore be borne in mind that the afterpotentials, analysed here at room temperature, will not be as prominent under normal physiological conditions.

Response to injected current pulses

The electrical characteristics of the axon were examined by injecting current pulses through the electrode. The responses of an axon to a series of graded hyperpolarizing and depolarizing pulses are superimposed in Fig. 6. This shows that the response in both directions of voltage change was characterized by a series of components similar to those following the action potential. There was a prolonged "creep" of the voltage response to injected current and no plateau potential was reached by the short pulses used here. When the voltage was measured arbitrarily at the end of the short pulse and plotted

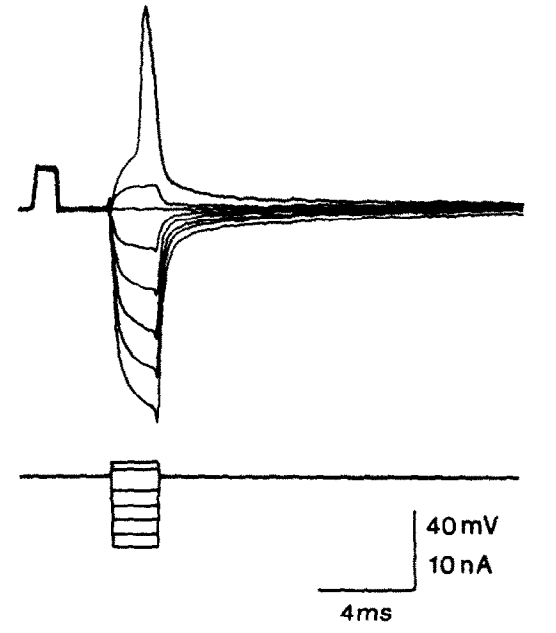

Fig. 6. The response of an axon to hyperpolarizing and depolarizing current pulses injected through the recording electrode. The voltage (upper trace) and current (lower trace) are shown superimposed for a series of responses. Note the presence of symmetrical negative and positive afterpotentials following the pulses and the action potential. The relation between voltage attained and current injected is essentially linear in this range, although the current pulse is too short to measure the input resistance.

against the injected current, a linear relation was found between the two. The slope of this line does not of course represent the input resistance of the axon for maintained currents, which would have to be measured with long pulses. Given the problems of impalement in these axons, such measurements were not made, as the input resistance measurement would be artefactually low. However, the action potential mechanism is also not involved directly with the input resistance of the axon because of the short duration of current flow. The input impedance at high frequency is more relevant to the axonal physiology.

When the rising (off) phase of the response to a short hyperpolarizing pulse was inverted and analysed in the same way as the action potential, by semilog plots, it was found possible to divide it into a series of components similar to those following the action potential (Fig. 7). When the pulse length was increased the same components were present, but their amplitudes were correspondingly increased. The response of an axon to a propagated action potential and the response to a hyperpolarizing current pulse were compared by inverting and superimposing one on the other (Fig. 8), and it was found that afterpotential amplitudes similar to those of the spike were produced by injecting hyperpolarizing current pulses that were considerably longer than the spike.

This has to be interpreted in the light of the fact that the action potential rapidly charges the whole length of the axon to similar potentials by distributed current injection, whereas point injection of current through the electrode produces a displacement of potential that declines exponentially from the point of impalement. The potential on a homogeneous, infinite cable declines as an error function rather than an exponential.[21,25] The situation in the finite myelinated axon is more complex than this, because the driving potential produced by current injection into the myelinated internode is much larger than the potential generated on the axolemmal cable itself. In practice, it was found that the potential at the injection site tended towards a final exponential decline, though the semilogarithmic slope of the hyperpolarizing response was steeper than that of the spike afterpotential (Fig. 8, inset). For nine axons in which the values were compared directly, the ratio of the final slopes of spike and 2 ms pulse were 0.56 ± 0.17.

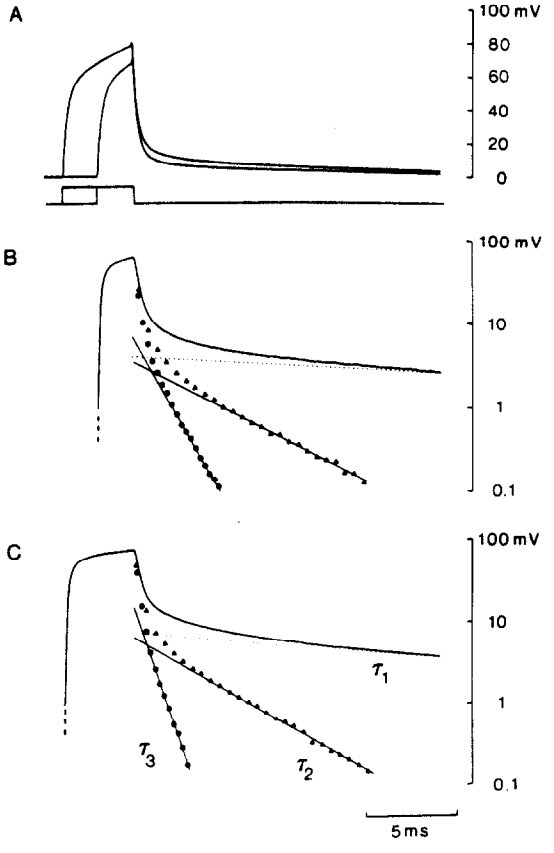

Fig. 7. The time constants of the rising (off) phase of the response to injected hyperpolarizing current were determined for two pulses of different duration, using the same technique as for the action potential in Fig. 2. (A) The two responses (negative up) and the associated current pulses, superimposed relative to the trailing edges. (B, C) Semilogarithmic plots of the two pulses, separated into the three longest time constants for each (τ_{1-3}). Note that these exponentials still account for only a small proportion of the amplitude of the voltage response. The faster components were not measurable here because of the limited frequency response of the microelectrode recording. Calculated values of the time constants were: in (B) $\tau_1 = 23$ ms, $\tau_2 = 2.0$ ms, $\tau_3 = 1.1$ ms and in (C) $\tau_1 = 22$ ms, $\tau_2 = 3.5$ ms, $\tau_3 = 0.6$ ms.

Conduction velocity and axon caliber

An estimate of the size of axons impaled in the ventral tracts of isolated rat spinal cord was obtained by measurement of the conduction velocity. The delay between the beginning of a stimulus pulse and the rising phase of the action potential (at 10% of full amplitude) was determined while moving the stimulating electrode in 0.5 or 1 mm steps along the tract and maintaining the stimulus current just above threshold. The slope of the relationship between stimulating and recording electrode separation and the conduction delay was used to determine the conduction velocity. The slopes ranged between 14 and 28 m/s at 25°C in a sample of ten axons, with a mean of 21 m/s.

The relationship between conduction velocity and nerve fiber diameter is not clear for the central nervous system. At physiological temperature the relationship for large peripheral axons is generally accepted to be *ca* 6 m/s per micron of overall fiber diameter,[22] but the ratio is close to 4.5 in smaller peripheral axons[8] and this value appeared to be approximately applicable to central spinal axons in the cat.[5] This relation needs to be defined with higher resolution techniques, however, preferably with combined measurements in identified axons. It is reasonable to assume that the electrode selectively impaled the largest axons, consistent with the statistical probability of coaxial alignment (see Discussion in

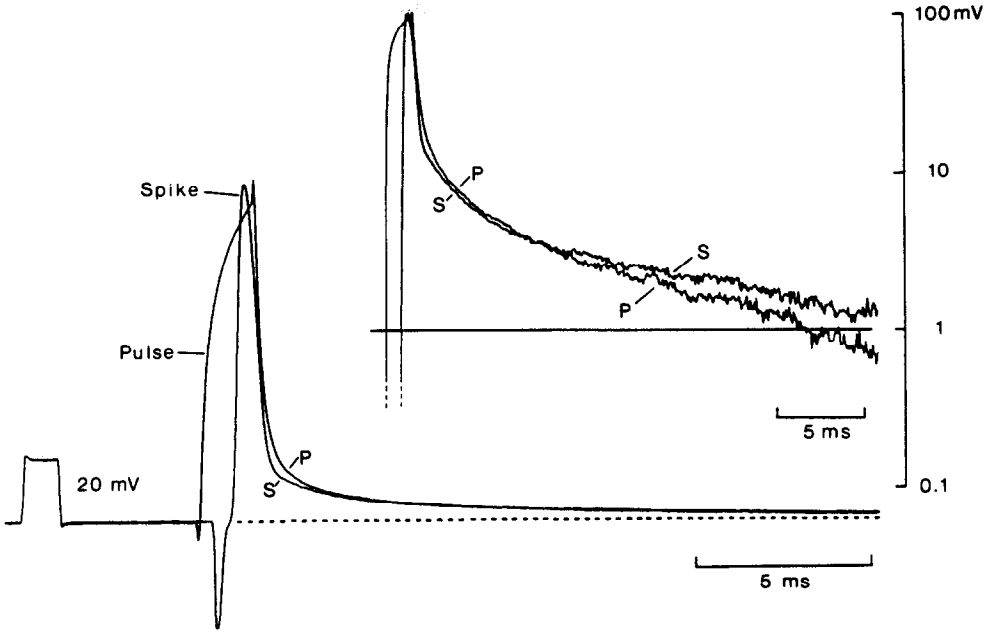

Fig. 8. A figure to compare the action potential with the response of the axon to injected current. A square hyperpolarizing current pulse of 2 ms duration was injected through the electrode. The voltage response of the axon was recorded, inverted (negative up) and superimposed on the record of an action potential initiated by a 0.5 ms depolarizing, threshold pulse. The same records are shown in a semilog plot (inset). The afterpotential of the spike (S) was similar in amplitude to the slow rising phase of the passive response to hyperpolarizing current, though the time-integrated voltage change associated with the pulse (P) was about twice that of the action potential. The semilog slope of the pulse was steeper than that of the spike—consistent with the point source of current injection. The earlier part of the falling phase is larger and slower for the pulse—consistent with the suggestion that this part of the afterpotential is generated near to the recording site.

Ref. 5). The largest axons in the rat ventral tracts were found to be of the order of 10 μm in glutaraldehyde-fixed material (i.e. axolemmal diameter only). The axons recorded in this study were therefore in the range of 5–10 μm dia.

Recordings from cat spinal cord

Qualitatively similar observations were made incidentally from cat spinal axons during the course of another study.[5] The chief quantitative difference noted in the cat was that the time constant of the afterpotential was larger than that for the rat, at 44 ± 17 ms, while the peak amplitude was similar at 4.0 ± 1.2 mV (mean $\pm$ SD, $n = 13$). This might represent a species difference, but it might also be related to difference in size , as the largest axons in the cat study were *ca* 15 μm dia, as opposed to 10 μm in the rat. The largest time constants in the cat axons were 80 ms, which is within the range of values reported for frog and lizard peripheral axons.[1] Other characteristics of action potential recordings in this small sample of cat axons were similar to those of the rat.

DISCUSSION

The afterpotential phenomenon described here for the mammalian central spinal axon appears qualitatively similar to that described for the vertebrate peripheral axon by Barrett and Barrett.[1] We agree with these investigators in interpreting the afterpotential as the result of passive capacitative discharge of the internodal axolemma. It is unlikely to result from ionic conductance changes or accumulation of periaxonal potassium, as it responds symmetrically to hyperpolarizing and depolarizing currents and shows the relation to current intensity and duration that would be expected of capacitance and resistance in parallel. The only structural element that appears capable of providing the large electrical capacitance and resistance necessary to generate the long time constants is the internodal axolemma.

Acceptance of this interpretation of the afterpotential requires the explanation of corollaries at variance with some previously accepted concepts and observations. Briefly stated, these corrolaries include the requirement that the resistance of the axolemma be relatively high, that the myelin sheath be of relatively low resistance and that the nodal leakage resistance be higher than values recorded in isolated fibers. Primarily we would like to know why the myelin sheath should be electrically leaky, when the compact myelin has long been considered the prime example of an insulating membrane. A similar question was examined in the paper by Barrett and Barrett,[1] on the assumption that some pathway between the myelin layers was reponsible for the current

leak, but there remain a number of inconsistencies between this interpretation and previously published data.

Corollaries of the afterpotential

The slowest component of the afterpotential in the central axon has a mean time constant of 25 ms in the rat. If we assume a 10 μm dia axon, which would be expected to have approximately a 1 mm internode length,[30] then the expected capacitance of the internodal axolemma is about 0.31 nF, using the generally accepted value of 1 μF/cm^2 for the capacitance of cell membranes.[25,42] The parallel resistance required to produce a time constant of 25 ms is then 80 MΩ, on the basis of the relation for capacitance and resistance in parallel: $\tau = R \times C$. But the myelinated axon is not a simple membrane cylinder, for which the longest time constant can be equated with the time constant of the membrane (τ_0 or τ_m).[25,35]

The resistance in parallel with the capacitance of the internodal axolemma includes not only the resistance of the axolemma itself but also the current path through the myelin sheath, the nodes and the axon core—as can be seen clearly in Fig. 9. The core resistance is low, being less than 10 MΩ for one half of the internode (R_{ax} in Fig. 9) and the membrane of the node is probably of lower specific resistance than that of the internode (see discussion below). If the capacitance of the internode charges to 4 mV during the passage of the action potential, the effective resistance of the myelin sheath must also be quite low. It will require 1.2 nA for 1 ms to charge 0.3 nF (the axolemmal capacitance) by 4 mV. Capacitative current flow through the myelin sheath will be brief, given the small capacitance to be expected of about 150 membranes stacked in series.[4] Subsequent flow of current into the axolemmal capacitance will be limited by the resistance of the sheath.

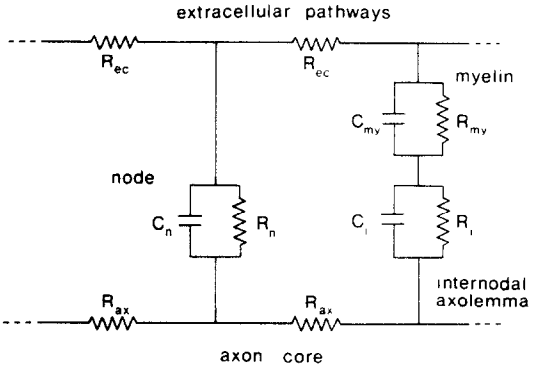

Fig. 9. A simplified representation of the passive electrical properties of basic unit of the myelinated fiber-node and internode. From the aspect of the afterpotential, the key element in this circuit is the capacitance of the internodal axolemma (C_i). The charge on this capacitance will be changed when the potential of the resting axon is changed, as by the passage of an action potential, but current flowing into C_i must pass through the capacitance or resistance of the myelin sheath (C_{my}, R_{my}). In the process of relaxation to the resting state, the transient charge on C_i can be dissipated both through the parallel resistance of the axolemma (R_i) and through the longer pathway of the myelin sheath (C_{my}, R_{my}), the extracellular space (R_{ec}), the nodal membrane (C_n, R_n), and the axon core (R_{ax}). A collection of such units joined end-to-end will represent the distributed R–C network of the fiber.

The action potential duration, measured in the myelin sheath was *ca* 0.8 ms at 25°C and the driving voltage across the myelin must average about 60 mV during the spike, given that the action potential amplitude is probably in the region of 120–130 mV,[24,31] that only 4 mV of this potential is developed across the axolemma and that the spike shape can be approximated to a triangle in form. The resistance of the myelin sheath required for passage of sufficient current to charge the axolemma is therefore about 40 MΩ (i.e. an average voltage of 60 mV divided by an average current of 1.5 nA for 0.8 ms). The current passing through the resistance of the axolemma will be small, given the necessary high resistance and the voltage drop of only 4 mV.

These values appear to be at variance with the data on current flow in isolated peripheral nerve fibers (e.g. Refs 23 and 50). This problem is discussed in the accompanying paper,[7] on the basis of quantitative predictions of a computer simulation.

The resistance of the nodal membrane

The resistances of the nodal and internodal membranes are the limiting factors in determining the time constant of the afterpotential. If the nodal leakage resistance were the 20–40 MΩ calculated from isolated peripheral fibers,[10,14,31] then it would not be possible to generate the required parallel resistance of 80 MΩ, even if the internodal axolemma were of infinite resistance. As time constants up to 80 ms are recorded in the mammal, while they are typically in excess of 100 ms in the amphibian,[1] it seems that the leakage conductance of the nodes is less *in situ* than the values obtained from isolated nodes have suggested. This may reflect a limitation of the voltage clamping technique. Data of Chiu and Ritchie[13] show that for large peripheral fibers of the frog, the leakage resistance of short length of central internode, recorded in the same way, can also be extremely low: from their Fig. 2(A), approximately 90 MΩ for a length of 50 μm, which is as short or shorter than the width of the recording pool containing the node in most clamping experiments. If the internodal component represents a leak of this magnitude then the estimation of nodal leakage conductance becomes quite difficult.

It is a striking fact that, if ultrastructural measurements[2,34] are accepted, then the area of the node is of the order of 25 μm^2. This means that the previously calculated 30–40 MΩ nodal resistance corresponds to a membrane resistance of only 7–12 Ω cm^2. If the observed nodal constriction results from artefactual shrinkage, then the area may be as much as 50 μm^2, but this would still involve a mem-

brane resistance of only 20 Ω cm^2, which remains unusually low. The observations of Williams and Hall[54] on paranodal swelling and retraction of myelin point to the possibility that values obtained from teased single peripheral fibres may not be representative of the *in situ* morphology or physiology. Against this may be placed the observations of Uhrik and Stampfli[52] that it is possible to maintain normal nodal morphology, at least for small fibers and short periods of time.

The resistance of the myelin sheath

To charge the internodal axolemma, current must pass along a relatively low resistance path through the myelin sheath. It is possible that this pathway involves circumventing the myelin lamellae themselves, utilizing some longitudinal cytoplasmic or extracellular route and a paranodal shunt. The possibilities for such a pathway were considered extensively by Barrett and Barrett,[1] though even with the most generous allowances for the cross-sectional area of such pathways it was not possible to identify a suitable candidate. In fact the potential for low-resistance longitudinal pathways was probably overestimated, given that most of the ultrastructural data in the literature refers to small-diameter axons (because they are easier to fix satisfactorily and to display photographically at high magnification). The periaxonal space is too narrow to provide such a pathway.[2,19] A separation of 10–20 nm around a 10 μm axon would have a longitudinal resistance of about 4–8 MΩ/μm. A possible pathway exists in the inner loop of the cytoplasm of the myelin sheath. In the smallest axons this loop can have a cross-sectional area that is a significant proportion of the area of the axon itself but, for larger axons, the size of this loop does not increase substantially. It is so small as to be barely distinguishable in micrographs that demonstrate the whole axon cross section. This appears to be the case both in peripheral and central axons[3,4] though large central axons are rarely illustrated because of the difficulty of fixation.

Given that the longitudinal core resistance of the internodal axon is about one half of the resistance required of the whole "leakage pathway", it seems unreasonable to suggest that a longitudinal pathway of sufficiently low resistance is somehow hidden by fixation artefacts or by our incomplete knowlege of the structure of the myelin sheath. The less intuitively appealing, but apparently necessary, interpretation is that the myelin lamellae themselves are of low resistance. This seems to contradict the apparent specialization of the myelin structure for an insulating role, with a low protein content, the stacking together of multiple lipid layers and the specialized junctions at the paranodal loops. However, the myelin membranes clearly contain proteins and distinct membrane particles[44] that may be the substrates of hydrophylic channels. There is even evidence of distinct radial structures in the central myelin sheath that could represent the alignment of such channels.[32,33,38] As yet we have no means of determining the electrical properties of membranes from their ultrastructural appearance and there are no direct measurements of the resistivity of compact myelin. The apparent specialization of the myelin sheath can be adequately explained by the necessity for a capacitative shield on the internode. This also requires the stacking of mutiple membranes, and a close paranodal seal to the axolemma. The membrane resistances of glial cells can be low relative to those of most neurons,[48] and the membrane resistance required to produce a resistance of 40 MΩ in the myelin sheath would be about 100 Ω cm^2, which is within the range estimated for astroglial cells.

The problem of axolemmal capacitance

The interpretation given above depends critically on the assumption that the internodal axolemma represents a capacitance of the order of 1 μF/cm^2. If it should have a smaller capacitance than this, then the current flow though the myelin sheath required to produce the observed potential would be correspondingly less. A possible substrate for a lower capacitance exists in the fact that the axolemma is closely associated with the inner membrane of the myelin sheath (reviewed in Ref. 19). It is possible that this double membrane might combine to produce a unit with one half the capacitance of the axolemma alone. Unfortunately this alternative explanation would require an equivalently higher parallel resistance to restore the time constant of discharge to the observed value, and the additional hypotheses would not help us to reconcile the data, unless the resistance of the inner membrane of the myelin is found to be much higher than that of the rest of the sheath. If the inner membrane has a resistance similar to the rest of the myelin, it would not significantly affect the electrical behaviour of the system. Nevertheless, the possibility of a specialized physiology of this membrane association should be kept in mind for further studies.

Faster components of the afterpotential

The observations reported here differ qualitatively from those in the peripheral axon[1] in the existence of larger amplitude and faster components superimposed on the long afterpotential. It is possible to explain these components by assuming that the microelectrode produces an additional leakage conductance in the myelin sheath at the site of impalement. This is a reasonable assumption, given that some leakage is produced in the axon itself and that penetration of the myelin is not merely by the end of the electrode but by several microns of its tapered tip. The difference from the peripheral axon data may result from a difference of electrode properties or represent a real difference in the reaction of mammalian central myelin and amphibian and reptilian peripheral myelin to impalement. Preliminary data from mammalian peripheral axons indicate that some

of the difference is due to differences in central and peripheral myelin. These two membrane types have different molecular structures, and different cellular origins. The central myelin sheath is less stabilized by aldehyde fixatives, for example, and tends to rapidly lose its lamellar organization.[12] Spinal cord myelin may be particularly unstable.[47]

Significance of current leakage at impalement

The presence of a leakage pathway around the recording electrode will affect the recorded potentials in predictable ways. The primary effect will be depolarization at the impalement site, but this can be offset by current injection through the microelectrode. Secondary effects include an attenuation of the action potential and the appearance of shorter duration components of the afterpotential. The following paper[7] shows that the existence of an additional leakage conductance at the site of recording has little effect on the longer component of the afterpotential, beyond a slight reduction in amplitude and time constant, nor does it profoundly affect interpretation of the electrical origin of the afterpotential.

data and those from lower vertebrate peripheral nerves[1] are that the time constant of the afterpotential in the rat is less than 25% of that in the amphibian at similar temperature, and the maximum amplitude of charge is less than half. Initial data from the cat spinal cord show an intermediate time constant—approximately twice that of the rat and half that of frog and lizard. This suggests that there may be interspecific variations in axolemmal and myelin resistances, though these differences may reflect fiber size or fiber type, given the small samples involved. Differences between vertebrate classes may also be related to the normal operating temperature, as well as to the presence of a more prominent voltage-dependent potassium conductance in the amphibian node of Ranvier, which plays some part in the repolarizing phase of the action potential, at least in large axons.[16,46]

The shorter time constant of the mammalian afterpotential is paralleled by the shorter time course of the superexcitable period in mammalian spinal axons[40,26] compared with amphibian peripheral axons.[37] It is likely that the presence of the afterpotential is at least partly responsible for the decrease in threshold of the axon following an action potential, as suggested by Barrett and Barrett.[1] It also appears that the amplitude of the superexcitable effect may be less in the mammalian axon, in agreement with the smaller amplitude of the afterpotential, though the mammalian studies have not yet been carried out to the same degree of precision nor at a temperature comparable to the amphibian studies.

Modelling and interpretation

The interpretation given above is explored further in the following paper,[7] which examines the behaviour of a mathematical model of the myelinated axon. This helps to explain how the observed potentials may be generated, and why they may have evolved.

Acknowledgements—This study was supported by grants NS 10164 and NS 15590 from NIH, NINCDS.

REFERENCES

1. Barrett E. F. and Barrett J. N. (1982) Intracellular recording from myelinated axons: mechanism of the depolarizing afterpotential. *J. Physiol., Lond.* **323,** 117–144.
2. Berthold C.-H. (1978) Morphology of normal peripheral axons. In *Physiology and Pathobiology of Axons* (ed. Waxman S. G.), pp. 3–63. Raven Press, New York.
3. Berthold C.-H. and Carlstedt T. (1977) Observations on the morphology at the transition between the peripheral and the central nervous system in the cat. II. General organization of the transitional region in S1 dorsal rootlets. *Acta physiol. scand.* Suppl. 446, 23–32.
4. Berthold C.-H. and Carlstedt T. (1977) Observations on the morphology at the transition between the peripheral and the central nervous system in the cat. III. Myelinated fibers in S1 dorsal rootlets. *Acta physiol. scand.* Suppl. 446, 43–60.
5. Blight A. R. (1983) Axonal physiology of chronic spinal cord injury in the cat: intracellular recording *in vitro*. *Neuroscience* **10,** 1471–1486.
6. Blight A. R. and Someya S. (1983) Action potentials of mammalian central spinal axons *in vitro*: depolarizing afterpotentials and the role of the myelin sheath. *Soc. Neurosci. Abstr.* **9,** 505.
7. Blight A. R. (1985) Computer simulation of action potentials and afterpotentials in mammalian myelinated axons: the case for a lower resistance myelin sheath. *Neuroscience* **15,** 13–31.
8. Boyd I. A. and Kalu K. U. (1979) Scaling factor relating conduction velocity and diameter for myelinated afferent nerve fibers in the cat hindlimb. *J. Physiol., Lond.* **289,** 277–297.
9. Brill M. H., Waxman S. G., Moore J. W. and Joyner R. W. (1977) Conduction velocity and spike configuration in myelinated fibers: computed dependence on internode distance. *J. Neurol. Neurosurg. Psychiat.* **40,** 769–774.
10. Brismar T. (1980) Potential clamp analysis of membrane currents in rat myelinated nerve fibers. *J. Physiol., Lond.* **298,** 171–184.
11. Brismar T. (1981) Electrical properties of isolated demyelinated rat nerve fibers. *Acta physiol. scand.* **113,** 161–166.
12. Carlstedt T. (1977) Observations on the morphology at the transition between the peripheral and the central nervous system in the cat. I. A preparative procedure useful for electron microscopy of the lumbosacral dorsal rootlets. *Acta physiol. scand.* Suppl. 446, 5–21.

13. Chiu S. Y. and Ritchie J. M. (1982) Evidence for the presence of potassium channels in the internode of frog myelinated nerve fibers. *J. Physiol., Lond.* **322,** 485–501.
14. Chiu S. Y., Ritchie J. M., Rogart R. B. and Stagg D. (1979) A quantitative description of membrane currents in rabbit myelinated nerve. *J. Physiol., Lond.* **292,** 149–166.
15. Fitzhugh R. (1962) Computation of impulse initiation and saltatory conduction in a myelinated nerve fiber. *Biophys. J.* **2,** 11–21.
16. Frankenhaeuser B. and Huxley A. F. (1964) The action potential in the myelinated nerve fiber of *Xenopus laevis*, as computed on the basis of voltage clamp data. *J. Physiol., Lond.* **171,** 302–315.
17. Goldman L. and Albus J. S. (1968) Computation of impulse conduction in myelinated fibers: theoretical basis of the velocity–diameter relation. *Biophys. J.* **8,** 596–607.
18. Hille B. (1977) Ionic basis of resting and action potentials. In *Handbook of Physiology*, Section 1. *The Nervous System*, Vol. 1, Part 1 (ed. Kandel E. R.), pp. 99–136. American Physiological Society, Bethesda, Maryland.
19. Hirano A. (1983) Reaction of the periaxonal space to some pathological processes. In *Progress in Neuropathology*. Vol I. (ed. Zimmerman H. M.), pp. 99–112. Raven Press, New York.
20. Hodgkin A. L. (1964) *The Conduction of the Nervous Impulse*. Liverpool University Press.
21. Hodgkin A. L. and Rushton W. A. H. (1946) The electrical constants of a crustacean nerve fibre. *Proc. R. Soc. Ser B* **133,** 444–479.
22. Hursh J. B. (1939) Conduction velocity and diameter of nerve fibers. *Am. J. Physiol.* **127,** 131–139.
23. Huxley A. F. and Stampfli R. (1949) Evidence for saltatory conduction in peripheral myelinated nerve fibres. *J. Physiol., Lond.* **108,** 315–339.
24. Huxley A. F. and Stampfli R. (1951) Direct determination of membrane resting potential and action potential in single myelinated nerve fibres. *J. Physiol., Lond.* **112,** 476–495.
25. Jack J. J. B., Noble D. and Tsien R. W. (1975) *Electric Current Flow in Excitable Cells*. Oxford University Press, Oxford.
26. Kocsis J. D. and Waxman S. G. (1981) Action potential electrogenesis in mammalian central axons. In *Demyelinating Diseases: Basic and Clinical Electrophysiology* (eds Waxman S. G. and Ritchie J. M.), pp. 299–312, Raven Press, New York.
27. Koles Z. J. and Rasminsky M. (1972) A computer simulation of conduction in demyelinated nerve fibres. *J. Physiol., Lond.* **227,** 351–364.
28. Llinás R. and Sugimori M. (1980) Electrophysiological properties of *in vitro* Purkinje cell somata in mammalian cerebellar slices. *J. Physiol., Lond.* **305,** 171–195.
29. Moore J. W., Joyner R. W., Brill M. H., Waxman S. and Najar-Joa M. (1978) Simulations of conduction in uniform myelinated fibers. Relative sensitivity to changes in nodal and internodal parameters. *Biophys. J.* **21,** 147–160.
30. Murray J. A. and Blakemore W. F. (1980) The relationship between internodal length and fibre diameter in the spinal cord of the cat. *J. neurol. Sci.* **45,** 29–41.
31. Neumcke B. and Stampfli R. (1982) Sodium current fluctuations in rat myelinated nerve fibres. *J. Physiol., Lond.* **329,** 163–184.
32. Peters A., Palay S. L. and Webster H. de F. (1976) *The Fine Structure of the Nervous System*. W. B. Saunders, Philadelphia.
33. Pinto da Silva P. and Miller R. G. (1975) Membrane particles on fracture faces of frozen myelin. *Proc. natn. Acad. Sci. U.S.A.* **72,** 4046–4050.
34. Raine C. S. (1982) Differences between the nodes of Ranvier of large and small diameter fibres in the P.N.S. *J. Neurocytol.* **11,** 935–947.
35. Rall W. (1969) Time constants and electrotonic length of membrane cylinders and neurons. *Biophys. J.* **9,** 1483–1508.
36. Ranvier M. L. (1878) *Lecons sur l'Histologie du Systeme Nerveux*. Librairie F. Savy, Paris.
37. Raymond S. A. (1979) Effects of nerve impulses on threshold of frog sciatic nerve fibres. *J. Physiol., Lond.* **290,** 273–303.
38. Reale E., Luciano L. and Spitznas M. (1975) Zonulae occludentes of the myelin lamellae in the nerve fibre layer of the retina and in the optic nerve of the rabbit: a demonstration by the freeze fracture method. *J. Neurocytol.* **4,** 131–140.
39. Ritchie J. M. and Rogart R. B. (1977) The density of sodium channels in mammalian myelinated nerve fibres and the nature of the axonal membrane under the myelin sheath. *Proc. natn. Acad. Sci. U.S.A.* **74,** 211–215.
40. Rudin J. M. and Eisenman G. (1954) The action potential of spinal axons *in vitro*. *J. gen. Physiol.* **37,** 505–538.
41. Rushton W. A. H. (1951) A theory of the effects of fibre size in medullated nerve. *J. Physiol., Lond.* **115,** 101–122.
42. Schanne O. F. and Ruiz P.-Ceretti E. (1978) *Impedance Measurement in Biological Cells*. John Wiley, New York.
43. Schauf C. L. and Davis F. A. (1974) Impulse conduction in multiple sclerosis: a theoretical basis for modification by temperature and pharmacological agents. *J. Neurol. Neurosurg. Psychiat.* **37,** 152–161.
44. Schnapp B. and Mugnaini E. (1978) Membrane architecture of myelinated fibres as seen by freeze-fracture. In *Physiology and Pathobiology of Axons* (ed. Waxman S. G.), pp. 83–123. Raven Press, New York.
45. Smith R. S. and Koles Z. J. (1970) Myelinated nerve fibres: computed effect of myelin thickness on conduction velocity. *Am. J. Physiol.* **219,** 1256–1258.
46. Smith K. J. and Schauf C. L. (1981) Size-dependent variation of nodal properties in myelinated nerve. *Nature* **293,** 297–299.
47. Smith M. E. and Sedgewick L. M. (1975) Studies of the mechanism of demyelination. Regional differences in myelin stability *in vitro*. *J. Neurochem.* **24,** 763–770.
48. Somjen G. G. (1975) Electrophysiology of neuroglia. *A. Rev. Physiol.* **37,** 163–190.
49. Stampfli R. and Hille B. (1976) Electrophysiology of peripheral myelinated nerve. In *Frog Neurobiology. A Handbook* (eds Llinás R. and Precht W.), pp. 3–32. Springer, New York.
50. Tasaki I. (1955) New measurements of the capacity and the resistance of the myelin sheath and the nodal membrane of the isolated frog nerve fiber. *Am. J. Physiol.* **181,** 639–650.
51. Tasaki I. (1968) *Nerve Excitation. A Macromolecular Approach*. Thomas, Illinois.
52. Uhrik B. and Stampfli R. (1981) Ultrastructural observations on nodes of Ranvier from isolated single frog peripheral nerve fibres. *Brain Res.* **215,** 93–101.
53. Waxman S. G. and Brill M. H. (1978) Conduction through demyelinated plaques in multiple sclerosis: computer simulations of facilitation by short internodes. *J. Neurol. Neurosurg. Psychiat.* **41,** 408–417.

54. Williams P. L. and Hall S. M. (1971) Prolonged *in vivo* observations of normal peripheral nerve fibres and their acute reactions to crush and deliberate trauma. *J. Anat.* **108,** 397–408.
55. Woodbury J. W. (1952) Direct membrane resting and action potentials from single myelinated nerve fibers. *J. cell. comp. Physiol.* **39,** 323–339.
56. Yamamoto C. and McIlwain H. (1966) Electrical activities in thin sections from the mammalian brain maintained in chemically-defined media *in vitro*. *J. Neurochem.* **13,** 1333–1343.

(*Accepted* 11 *November* 1984)